ARTHRITIS & RHEUMATISM
Vol. 62, No. 5, May 2010, 1224–1235
DOI 10.1002/art.27395

Inhibition of Fibroblast Activation Protein and Dipeptidylpeptidase 4 Increases Cartilage Invasion by Rheumatoid Arthritis Synovial Fibroblasts

Caroline Ospelt, Joachim C. Mertens, Astrid Jüngel, Fabia Brentano, Hanna Maciejewska-Rodriguez, Lars C. Huber, Hossein Hemmatazad, Thomas Wüest, Alexander Knuth, Renate E. Gay, Beat A. Michel, Steffen Gay, Christoph Renner, and Stefan Bauer

Objective. **Since fibroblasts in the synovium of patients with rheumatoid arthritis (RA) express the serine proteases fibroblast activation protein (FAP) and dipeptidylpeptidase 4 (DPP-4)/CD26, we undertook the current study to determine the functional role of both enzymes in the invasion of RA synovial fibroblasts (RASFs) into articular cartilage.**

Methods. **Expression of FAP and DPP-4/CD26 by RASFs was analyzed using fluorescence-activated cell sorting and immunocytochemistry. Serine protease activity was measured by cleavage of fluorogenic substrates and inhibited upon treatment with L-glutamyl L-boroproline. The induction and expression of matrix metalloproteinases (MMPs) and tissue inhibitors of metalloproteinases (TIMPs) in RASFs were detected using real-time polymerase chain reaction. Densitometric measurements of MMPs using immunoblotting confirmed our findings on the messenger RNA level. Stromal cell–derived factor 1 (SDF-1 [CXCL12]), MMP-1, and MMP-3 protein levels were measured using enzyme-linked immunosorbent assay. The impact of FAP and DPP-4/CD26 inhibition on the invasiveness of RASFs was analyzed in the SCID mouse coimplantation model of RA using immunohistochemistry.**

Results. **Inhibition of serine protease activity of FAP and DPP-4/CD26 in vitro led to increased levels of SDF-1 in concert with MMP-1 and MMP-3, which are downstream effectors of SDF-1 signaling. Using the SCID mouse coimplantation model, inhibition of enzymatic activity in vivo significantly promoted invasion of xenotransplanted RASFs into cotransplanted human cartilage. Zones of cartilage resorption were infiltrated by FAP-expressing RASFs and marked by a significantly higher accumulation of MMP-1 and MMP-3, when compared with controls.**

Conclusion. **Our results indicate a central role for the serine protease activity of FAP and DPP-4/CD26 in protecting articular cartilage against invasion by synovial fibroblasts in RA.**

Rheumatoid arthritis (RA) is an inflammatory disease of unknown etiology and is characterized by progressive invasion of synovial fibroblasts into the articular cartilage and erosion of the underlying bone, leading to joint destruction (1). The major extracellular proteolytic enzymes involved in cartilage resorption are matrix metalloproteinases (MMPs) and serine proteases (2). Among them, dipeptidylpeptidase 4 (DPP-4), also designated as CD26, and fibroblast activation protein (FAP) are type II transmembrane glycoproteins with

Supported in part by the European Union Sixth Framework Programme Project AutoCure, the European Union Seventh Framework Programme Project Masterswitch, and the Institute of Arthritis Research, Epilanges, Switzerland. Drs. Jüngel and Renner's work was supported by the Swiss National Fund (grants SNF 320030-116842 and SNF 310000-120024/1, respectively).

Caroline Ospelt, MD, Joachim C. Mertens, MD, Astrid Jüngel, PhD, Fabia Brentano, PhD, Hanna Maciejewska-Rodriguez, MD, Lars C. Huber, MD, Hossein Hemmatazad, MD, Thomas Wüest, PhD, Alexander Knuth, MD, Renate E. Gay, MD, Beat A. Michel, MD, Steffen Gay, MD, Christoph Renner, MD, Stefan Bauer, MD: University Hospital, Zurich, Switzerland.

Drs. Renner and Bauer contributed equally to this work.

Drs. Renner and Bauer have a patent pending for the expression of fibroblast activation protein by rheumatoid myofibroblast-like synoviocytes.

Address correspondence and reprint requests to Stefan Bauer, MD, National Centre for Tumor Diseases, Department of Medical Oncology, University of Heidelberg, Im Neuenheimer Feld 350, 69120 Heidelberg, Germany. E-mail: stefan.bauer@nct-heidelberg.de.

Submitted for publication May 12, 2009; accepted in revised form February 4, 2010.

extracellular proteolytic activity (3,4). Both enzymes are members of the prolyl peptidase family cleaving N-terminal dipeptides from polypeptides with proline or alanine in the penultimate position and have been linked to several diseases, including epithelial cancers and arthritis (5).

DPP-4/CD26 is constitutively expressed by several cell types, including fibroblasts, endothelial and epithelial cells, leukocyte subsets, T lymphocytes, and macrophages. A small proportion of DPP-4/CD26 circulates as soluble protein in the blood. Its enzymatic activity depends on homodimerization of 110-kd subunits or on heterodimerization with other prolyl peptidase family members (6). In RA, the functional role of DPP-4/CD26 has not been conclusively defined and may depend on cell type– and compartment-specific expression. The number of peripheral T lymphocytes expressing DPP-4/CD26 is increased in the blood of RA patients (7). In contrast, the enzymatic activity and the protein levels of DPP-4/CD26 are decreased in sera and in synovial membranes from RA patients as compared with those from healthy controls (8,9). In addition, DPP-4/CD26 proteolytic activity is significantly lower in RA synovial fluid than in osteoarthritis synovial fluid (10,11).

In addition to the presence of DPP-4/CD26 in RA, FAP is strongly expressed in the rheumatoid synovium (12) and has been detected under conditions that promote cartilage resorption (13). Furthermore, the area of FAP-expressing RA synovial fibroblasts (RASFs) has been characterized as the center of high inflammatory activity in the RA synovium (12). FAP is a homodimer of 97-kd subunits, and the soluble form of FAP is termed "a2-antiplasmin cleaving enzyme" (14). FAP is structurally very similar to DPP-4/CD26 (15) but typically does not present in normal adult tissue (4). In addition to being detected in RASFs, FAP is expressed on activated fibroblasts associated with the granulation tissue in healing wounds, desmoplastic reaction, and the stroma of epithelial cancers (16). The morphologic predominance of FAP at the invadopodia of migrating fibroblasts further emphasizes a role in the remodeling of extracellular matrix (ECM) (17). This is underlined by the fact that FAP has both collagenolytic and gelatinolytic properties in addition to its "DPP-4–like activity," the term used herein to describe the integrated enzymatic activity of FAP and DPP-4. Among the prolyl peptidase family members, FAP exclusively cleaves denatured type I collagen as the principal protein component of ECM (18). However, the mechanistic role of FAP in pathologic processes promoting ECM degradation, and especially in RA, is unknown.

Recent data demonstrate that FAP only digests partially degraded or denatured type I collagen, thereby indicating an essential initial role for other enzymes (19). Indeed, several cytokines, chemokines, growth factors, and hormones share the penultimate proline or alanine motif, and their N-terminal truncation regulates bioactivity and function (20). However, the biologic relevance of FAP's membrane-bound, DPP-4–like activity is not precisely defined, since its natural substrate is still unknown. In addition, the impact of FAP's proteolytic activity on cartilage degradation remains unclear, since the degradation of type II collagen, the major protein constituent of cartilage, by FAP has not yet been reported. In the present study we addressed these issues by analyzing the influence of simultaneous modulation of both FAP-and DPP-4–related prolyl peptidase activity on the proinvasive profile of human RASFs.

MATERIALS AND METHODS

Ethics approval. Animal experiments and human sample collection were approved by the Swiss veterinary office and the Swiss ethics commission, respectively.

Cell culture. Synovial tissue was obtained from patients with RA diagnosed according to the American College of Rheumatology (formerly, the American Rheumatism Association) criteria for RA (21) who underwent joint replacement surgery. Data on patient characteristics are available online at http://www.klinikum.uni-heidelberg.de/fileadmin/NCT/PDF/PubLinks_NCT_SB_2009-10.pdf. After mincing, tissue was digested in 150 mg/ml Dispase II (Roche) for 60 minutes at 37°C. The cell suspension obtained was grown in Dulbecco's modified Eagle's medium (DMEM; Gibco Invitrogen) supplemented with 10% heat-inactivated fetal calf serum (FCS), 50 IU/ml penicillin/streptomycin with 0.2% fungicide, 2 m*M* L-glutamine, and 10 m*M* HEPES (all from Gibco Invitrogen). After 24 hours, only adherent cells were further cultured, and cells from passages 4–8 were used in experiments.

Flow cytometry (fluorescence-activated cell sorting [FACS]). RASFs were detached with Accutase (PAA Laboratories), washed with phosphate buffered saline (PBS)/1% FCS, and incubated with 10 μg/ml of anti-FAP (22) or with 0.2 μg/ml of anti-CD26 antibodies (Santa Cruz Biotechnology) for 30 minutes at 4°C. As a negative control, cells were incubated with respective concentrations of matched IgG isotypes. Cells were washed and subsequently incubated with fluorescein isothiocyanate–labeled mouse anti-rat or donkey anti-human IgG (both from Jackson ImmunoResearch) for 30 minutes at 4°C. Data were processed using CellQuest software (BD Biosciences).

Immunocytochemistry. Detached RASFs were seeded onto sterile histologic Superfrost Ultra Plus glass slides (Menzel-Gläser), grown to confluence, and fixed in methanol for 4 minutes at −20°C. Slides were blocked with 1% H_2O_2 and

1% bovine serum albumin (BSA)/5% goat serum and incubated overnight at 4°C, with or without mouse anti-human FAP antibodies (22). Primary antibodies were detected with horseradish peroxidase (HRP)–conjugated goat anti-mouse antibodies (Jackson ImmunoResearch) and visualized using aminoethylcarbazole (AEC) reagent.

Fluorogenic DPP-4–like activity assay. For enrichment of membrane proteins, RASFs (10^6) were resuspended in 50 m*M* Tris HCl, 150 m*M* NaCl buffer, pH 7.4, 2% (weight/volume) Triton X-114 and incubated on ice for 15 minutes. Cellular debris was removed by centrifugation (14,000 revolutions per minute for 5 minutes at 4°C). Supernatant was warmed for 10 minutes at 30°C, and phase separation was performed using centrifugation at room temperature. The detergent phase was washed with 1 ml reaction buffer (100 m*M* NaCl, 100 m*M* Tris, pH 7.8), phase-partitioned, and diluted 1:10 in reaction buffer. Diluted extracts were incubated with 0.5 m*M* Ala-Pro-7-amido-4-trifluoromethyl coumarin (Ala-Pro-AFC; Bachem) in 96-well plates at 37°C, and release of free AFC was measured using a Victor fluorescence reader (395 nm/530 nm; PerkinElmer Wallac), as described previously (23).

To measure enzymatic activity using immunoprecipitated FAP or DPP-4/CD26, RASFs (5×10^6) were solubilized in 5 ml lysis buffer (50 m*M* Tris HCl, 150 m*M* NaCl buffer, pH 7.4, 0.7% (w/v) β-octylglucopyranoside) by vortexing for 15 minutes at 4°C. Cell debris was removed by centrifugation, and the supernatant was incubated for 4 hours at 4°C with 50 μl protein A magnetic Dynabeads (Invitrogen) coated with either anti-human CD26 or anti-human FAP antibodies (22). Beads were removed from suspension using a magnetic rack, washed with PBS containing 0.1% Tween 20, diluted 1:10 in AFC reaction buffer (100 m*M* NaCl, 100 m*M* Tris, pH 7.8; Bachem), incubated with Ala-Pro-AFC, and measured. DPP-4–like activity was inhibited using L-glutamyl L-boroproline (PT-630; kindly provided by Point Therapeutics). PT-630 does not permeate cells and competitively inhibits extracellular dipeptidylpeptidases and structural homologs (50% inhibition concentration 2 n*M*) in a very selective manner (24). Daily dosing ensures the chemical knockout of dipeptidylpeptidase activity, since DPP-4 turnover is ~90 hours and enzyme activity remains inhibited at 80% for 48 hours after a single dose of PT-630. PT-630 was incubated with membrane extracts for 15 minutes prior to the addition of Ala-Pro-AFC substrate (25). Inhibition of DPP-4–like activity was measured as described above.

Inhibition of extracellular DPP-4–like activity. Prior to the inhibition experiments with PT-630, RASFs were starved for 24 hours with DMEM containing 0.5% FCS. PT-630 solutions were prepared according to the manufacturer's instructions and added to the cell culture medium (DMEM/0.5% FCS) every 24 hours at concentrations of 1 μ*M* and 1 n*M*.

RNA isolation, reverse transcription, and real-time polymerase chain reaction (PCR). Cells were lysed in RLT buffer, and total RNA was isolated using an RNeasy Mini kit (Qiagen), including a DNA digestion step using RNase-free DNase. Total RNA was reverse transcribed using random hexamers and MultiScribe reverse transcriptase (both from Applied Biosystems). Non–reverse-transcribed samples were used as negative controls. Single-reporter real-time PCR was performed using the ABI Prism 7700 Sequence Detection system (Applied Biosystems). Eukaryotic 18S ribosomal RNA, measured with a predeveloped primer/probe system (Applied Biosystems), served as endogenous controls for relative quantification. Fold differences were calculated as described previously (26). Primer sequences for MMPs and tissue inhibitors of metalloproteinases (TIMPs) have been published previously (27). Primer sequences for CXCL12, CD26, and FAP were as follows: for CXCL12, forward 5′-AGA-GCC-AAC-GTC-AAG-CAT-CT-3′ and reverse 5′-AGG-GCA-CAG-TTT-GGA-GTG-TT-3′; for CD26, forward 5′-CCG-TGG-TTC-TGC-TGA-ACA-AAG-3′ and reverse 5′-CTG-TCA-GCT-GTA-GCA-TCA-TCA-TC-3′; and for FAP, forward 5′-CAA-GAA-TGT-TTC-GGT-CCT-GT-3′ and reverse 5′-GTC-TGC-CAG-TCT-TCC-CTG-AA-5′. To exclude variances in the amplification, efficiency analysis was performed as described online at http://www3.appliedbiosystems.com/cms/groups/mcb_upport/documents/generaldocuments/cms_040980.pdf. The absolute value of the slope of log input amount versus ΔC_t (FAP-CD26) was 0.06.

Immunoblotting. Cultured RASFs were lysed in Laemmli buffer and boiled for 4 minutes. Equal volumes were loaded onto 10% gels and subjected to sodium dodecyl sulfate–polyacrylamide gel electrophoresis. Immunoblotting was performed using mouse anti-human MMP-1 (2 μg/ml; R&D Systems), mouse anti-human MMP-3 (2 μg/ml; Acris Antibodies), and mouse anti-human MMP-13 (2 μg/ml; R&D Systems) antibodies. After blotting proteins onto polyvinylidene fluoride membranes (Amersham GE Healthcare), membranes were blocked using 1% BSA (Sigma) for 1 hour at room temperature. Primary antibodies were incubated overnight at 4°C. Membranes were washed in Tris buffered saline/0.05% Tween 20 and incubated with HRP-conjugated goat anti-mouse IgG (Jackson ImmunoResearch) for 1 hour at room temperature. After repeated washes, bands were visualized using an ECL antibody detection kit and Hyperfilm ECL (both from Amersham GE Healthcare).

Enzyme-linked immunosorbent assay (ELISA). A DuoSet ELISA development kit (R&D Systems) was used to detect MMP-3 in cell supernatants. Antibodies in this kit recognize proMMP-3, mature MMP-3, and TIMP-complexed MMP-3. For the detection of proMMP-1 and active MMP-1, the SensoLyte MMP-1 ELISA kit (Anaspec) was used. Human stromal cell–derived factor 1 (SDF-1 [CXCL12]) was detected using a DuoSet ELISA development kit (R&D Systems).

SCID mouse model and inhibition of extracellular DPP-4–like activity in vivo. Healthy human cartilage was obtained from a patient undergoing joint replacement due to rotator cuff tear. The patient had no history of cartilage pathologies, and radiography revealed no signs of chondropathies. RASFs from passage 5 were trypsinized and added to pieces of sterile inert gel sponge (3–4-mm^3; Upjohn) at a concentration of 1×10^5 cells/sponge. The sponges and pieces of cartilage (1–2-mm^3) were implanted under the adipose capsule of the kidney in 4-week-old female SCID mice (Charles River). For substance administration by gavage, solutions of PT-630 were given orally twice daily over a period of 60 days at doses of 25 μg or 50 μg per mouse (28). The control group received only saline at the same volume (200 μl per gavage). After 60 days, mice were killed, blood was collected, and the implants were removed, fixed in 4% forma-

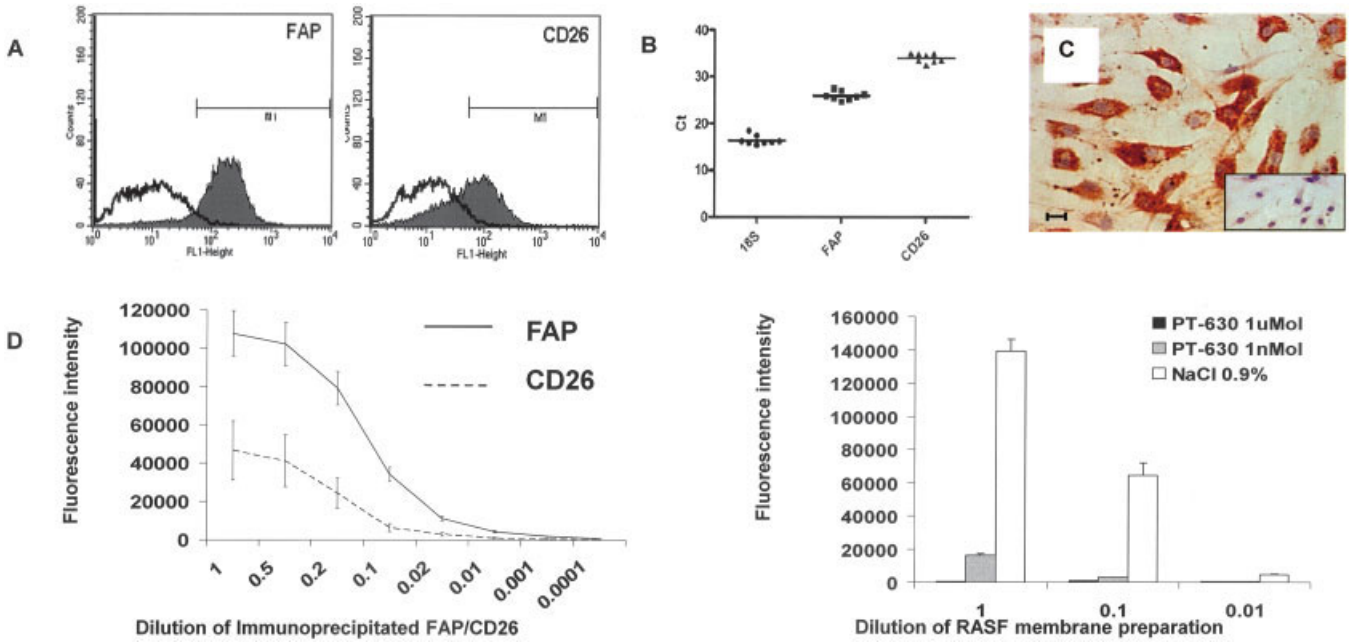

Figure 1. Rheumatoid arthritis synovial fibroblasts (RASFs) express fibroblast activation protein (FAP) and CD26 and exhibit dipeptidylpeptidase 4 (DPP-4)–like activity in RASFs. **A,** The expression of FAP and CD26 was measured in cultured RASFs by fluorescence-activated cell sorting analysis. Black lines with open areas represent negative controls, and black lines with solid gray areas represent positive cells. Results are representative of 3 experiments. **B,** Single-reporter real-time polymerase chain reaction was used to assess *FAP* and *DPP4*/*CD26* gene expression in cultured RASFs. Low C_t values represent high expression rates. Horizontal lines indicate the mean. **C,** Cell membrane expression of FAP was demonstrated by immunocytochemistry on covered slides. Bar = 10 μm. Irrelevant IgG was used as a negative control (**inset**) (original magnification × 100). **D,** DPP-4–like activity of FAP and CD26 immunoprecipitated from RASFs (5×10^6) was demonstrated upon cleavage of fluorogenic dipeptide substrate (Ala-Pro-7-amido-4-trifluoromethyl coumarin) (**left**), and attenuation of dipeptide hydrolysis was detected following incubation of dilutions of membrane preparations from RASFs (1×10^6) with control (NaCl) or with 1 n*M* or 1 μ*M* of L-glutamyl L-boroproline (PT-630) (**right**). Values are the mean and SEM (n = 4).

lin, and embedded in paraffin. Every 40 μm, a 4-μm–thick slide was mounted and stained with hematoxylin and eosin. Invasion of RASFs into cartilage was evaluated by two observers, who were blinded to the source of the implants, using a semiquantitative 5-point scale, as described previously (29).

Immunohistochemistry. Implants resected from SCID mice were either formalin-fixed and paraffin-embedded or were embedded in Tissue-Tek OCT compound (Sakura Finetek) and kept at −80°C. Paraffin-embedded slides were deparaffinized, pretreated in citrate buffer, and blocked with 1% H_2O_2, 1% BSA/5% goat serum. Slides were incubated overnight with 10 μg/ml mouse anti-human MMP-1 antibody (R&D Systems), 8.3 μg/ml mouse anti-human MMP-3 antibody, 4 μg/ml mouse anti-human prolyl 4-hydroxylase antibodies (both from Acris Antibodies), or respective concentrations of matched IgG isotypes (Dako). After washing with PBS/0.5% Tween 20, slides were incubated with biotinylated goat anti-mouse IgG (Jackson ImmunoResearch). The signal was amplified with HRP-conjugated streptavidin using a Vectastain Elite ABC kit (Vector), developed with AEC (Sigma-Aldrich), and counterstained with hematoxylin. Staining intensity was assessed on a semiquantitative 5-point scale, where 0 = absent, 1 = weak, 2 = moderate, 3 = high, and 4 = very high. Frozen slides were thawed at room temperature, fixed with acetone for 10 minutes at 4°C, air dried, and blocked with 0.1% H_2O_2, 1%BSA/5% goat serum. Slides were incubated with or without mouse anti-human FAP antibodies (22) overnight at 4°C. Primary antibodies were detected with HRP-conjugated goat anti-mouse antibodies (Jackson ImmunoResearch). Sections were developed with AEC and counterstained with hematoxylin.

Statistical analysis. Values are presented as the mean ± SEM. GraphPad Prism software was used for statistics and diagrams.

RESULTS

Synovial fibroblasts cultured from the synovium of RA patients express FAP and DPP-4/CD26. An association between FAP expression and arthritis is well established, and we have previously demonstrated that FAP is present on the surface of synovial fibroblasts in the lining layer of the synovium in RA patients (12). In the current study, we investigated surface expression of FAP (n = 5 patients) and DPP-4/CD26 (n = 8 patients) in cultured RASFs. As demonstrated using FACS ana-

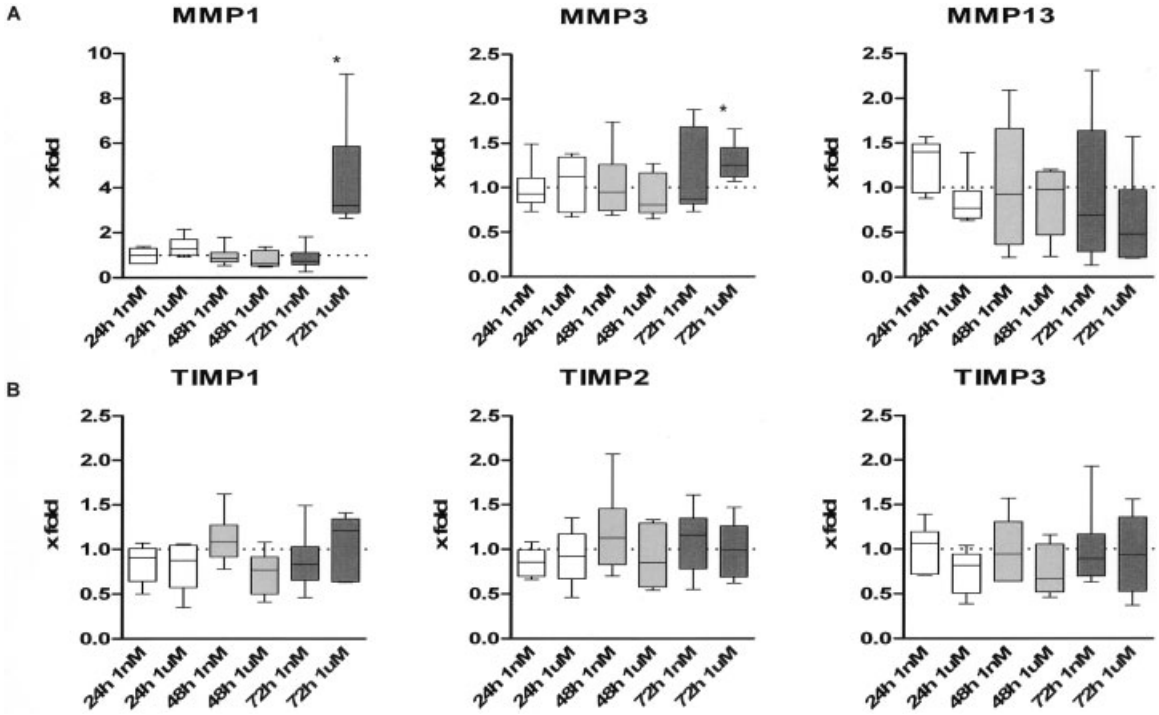

Figure 2. Inhibition of DPP-4–like activity induces the expression of matrix metalloproteinase 1 (MMP-1) and MMP-3 mRNA, but not MMP-13 mRNA or tissue inhibitor of metalloproteinases 1 (TIMP-1), TIMP-2, or TIMP-3 mRNA, in RASFs. Induction of MMP-1, MMP-3, and MMP-13 mRNA (**A**) and TIMP-1, TIMP-2, and TIMP-3 mRNA (**B**) was measured using real-time polymerase chain reaction after incubation with 1 n*M* or 1 μM of PT-630 for 24, 48, or 72 hours (n = 6 per condition), and levels were compared with those in noninhibited controls (basal level, defined as 1). Data are presented as box plots, where the boxes represent the 25th to 75th percentiles, the lines within the boxes represent the median, and the lines outside the boxes represent the minimum and maximum values. $* = P < 0.05$ versus basal level, by Wilcoxon's signed rank test. See Figure 1 for other definitions.

lysis, FAP was expressed on a mean ± SEM of 94 ± 1% of RASFs (Figure 1A), while DPP-4/CD26 was more variably expressed (46 ± 11% of RASFs [range 13–93%]) (Figure 1A). In addition, gene expression analysis revealed higher expression levels of *FAP* gene transcripts compared with levels of *DPP4*/*CD26* gene transcripts (Figure 1B). Immunohistochemical staining of monolayer cultures revealed the dense expression pattern of FAP, with IgG used as a negative control (Figure 1C).

FAP exhibits DPP-4–like activity on RASFs. FAP is capable of cleaving N-terminal Xaa-Pro sequences, and membrane extracts prepared from FAP-transfected cells specifically cleaved the fluorogenic substrate Ala-Pro-AFC (23). Membrane extracts prepared from RASFs (n = 4 patients) consistently exhibited DPP-4–like activity. Since DPP-4/CD26 is also integrated in the cell membrane of RASFs, we used immunoprecipitates to separate FAP from DPP-4/CD26, and we observed concentration-dependent individual peptidase activity of both FAP and DPP-4/CD26 immunoprecipitates (Figure 1D). DPPs can be inhibited by aminoboronic dipeptides, e.g., PT-630. This substance does not readily permeate cells, and its inhibiting function is restricted to the inhibition of extracellular enzymatic activity. Incubation of RASF membrane preparations with PT-630 prior to the addition of the fluorogenic substrate efficiently abrogated DPP-4–like activity (Figure 1D).

Inhibition of extracellular DPP-4–like activity of cultured RASFs increases CXCL12 and MMP levels in vitro. Serine proteases have been reported to be jointly involved in cell invasion and migration on a collagenous matrix in vitro (17). Since MMPs produced by RASFs play a major role in the destructive process in RA joints, we investigated whether modulation of extracellular DPP-4–like activity induces changes in the expression of MMP-1, MMP-3, and MMP-13. Expression levels of MMP-1, MMP-3, and MMP-13 messenger RNA

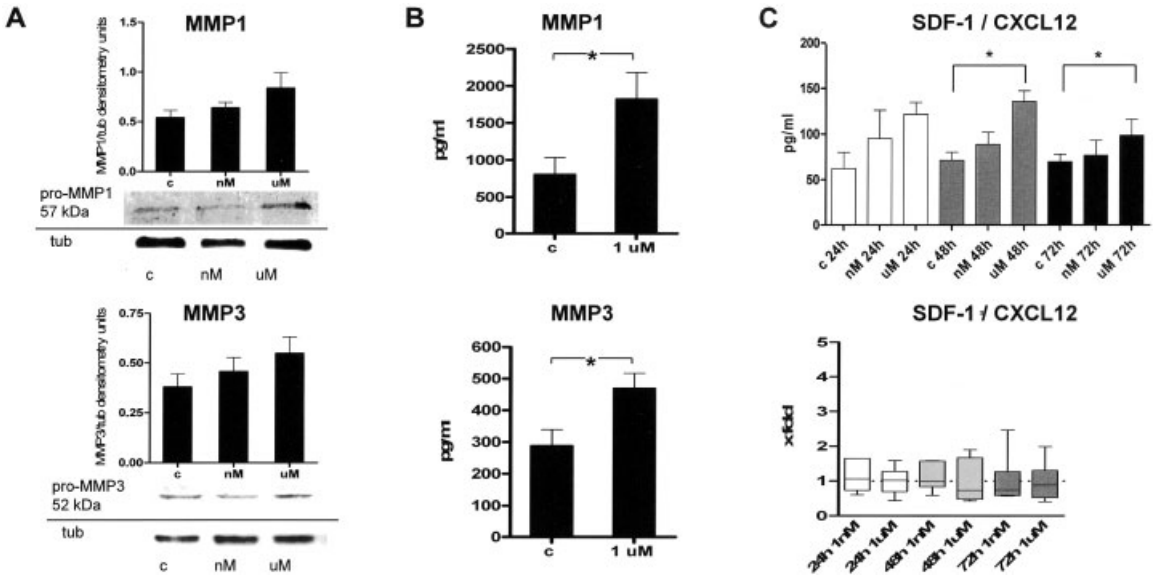

Figure 3. Inhibition of DPP-4–like activity induces matrix metalloproteinase 1 (MMP-1) and MMP-3 protein expression in RASFs and increases stromal cell–derived factor 1 (SDF-1) protein levels. **A,** After incubation with 1 n*M* or 1 μM of PT-630 (n = 5 per condition), intracellular levels of MMP-1 and MMP-3 were assessed in native RASFs using densitometry and immunoblotting, with α-tubulin (tub) used as a loading control. Values are the mean and SEM. **B,** Levels of secreted MMP-1 (n = 8) and MMP-3 (n = 7) in the supernatants of native (control [c]) RASFs and RASFs treated with 1 μM of PT-630 (n = 8) were measured by enzyme-linked immunosorbent assay (ELISA) after 72 hours. Values are the mean and SEM. $* = P <$ 0.05 by Wilcoxon's signed rank test. **C,** Release of SDF-1 (CXCL12) in the supernatants of cultured RASFs was measured by ELISA (n = 4) (**top**). Values are the mean and SEM. $* = P < 0.05$ by repeated-measures analysis of variance and Bonferroni's multiple comparison test. SDF-1 mRNA levels were assessed using single-reporter real-time polymerase chain reaction (n = 6) (**bottom**). Levels were measured after addition of 1 n*M* or 1 μM of PT-630 and in untreated control RASFs (basal level, defined as 1). Data are presented as box plots, where the boxes represent the 25th to 75th percentiles, the lines within the boxes represent the median, and the lines outside the boxes represent the minimum and maximum values. See Figure 1 for other definitions.

(mRNA) were not affected by incubation with PT-630 after 24 or 48 hours (n = 6). However, after 72 hours, expression of MMP-1 and MMP-3 mRNA was significantly increased when compared with expression levels in untreated cells (n = 6) (Figure 2A). Expression of MMP-1 mRNA was clearly increased (mean ± SEM 4.3 ± 1–fold) ($P = 0.02$), and although expression of MMP-3 mRNA was changed only slightly (1.3 ± 0.1–fold), this change was statistically significant ($P = 0.02$). Expression of MMP-13 mRNA remained unchanged (Figure 2A). No change in the expression of mRNA for the MMP inhibitors TIMP-1, TIMP-2, and TIMP-3 was observed at 24, 48, or 72 hours (n = 6 for each) (Figure 2B).

Densitometric measurements of MMP-1, MMP-3, and MMP-13 protein, as assessed using immunoblotting, were used to confirm the results observed on the mRNA level. Treatment with PT-630 (1 μM) for 72 hours resulted in a 56% increase in intracellular MMP-1 levels in RASFs (n = 5) versus controls (mean ± SEM MMP-1/tubulin densitometry units 0.54 ± 0.07 and 0.84 ± 0.15, respectively) (Figure 3A). Moreover, intracellular expression of MMP-3 was increased 45% in cells treated with PT-630 (n = 6) versus controls (MMP-3/tubulin densitometry units 0.38 ± 0.06 and 0.55 ± 0.08, respectively) (Figure 3A). Expression of MMP-13 was unchanged in cells treated with PT-630 (n = 3) versus untreated controls (MMP-13/tubulin densitometry units 0.23 ± 0.06 and 0.22 ± 0.02, respectively) (data not shown). Accordingly, 72 hours after the addition of PT-630, levels of secreted MMP-1 and MMP-3 were significantly higher, as measured by ELISA (Figure 3B). After exposure to 1 μM PT-630 for 72 hours, the mean ± SEM expression levels of MMP-1 increased from 802 ± 229 pg/ml in untreated RASFs (n = 8) to 1,824 ± 357 pg/ml, while expression levels of MMP-3 increased from 289 ± 51 pg/ml in untreated RASFs (n = 7) to 469 ± 48 pg/ml.

The delayed increase of MMPs upon inhibition of DPP-4–like activity suggested an indirect mechanism

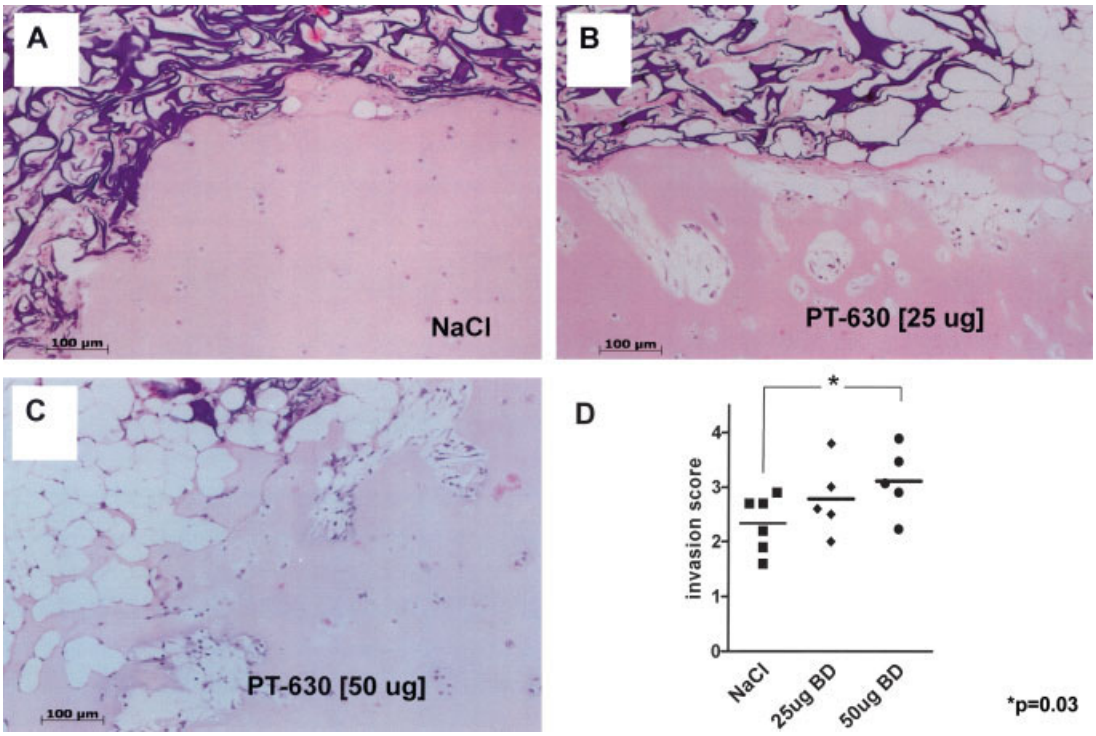

Figure 4. Inhibition of DPP-4–like activity enhances invasion of RASFs and cartilage destruction in the SCID mouse model. **A–C,** Hematoxylin and eosin–stained slides are representative of 6 control animals (**A**) and 5 animals treated with PT-630 (**B** and **C**). **D**, Invasion scores in controls and in mice treated with 25 μg BD PT-630 or 50 μg BD PT-630 were assessed. Mean $\pm$ SEM invasion scores were 2.3 $\pm$ 0.2 for controls, 2.8 $\pm$ 0.3 for mice treated with 25 μg PT-630 twice daily, and 3.1 $\pm$ 0.3 for mice treated with 50 μg PT-630 twice daily. Each symbol represents the overall invasion score of the implant taken from 1 mouse. Horizontal lines indicate the mean. See Figure 1 for definitions.

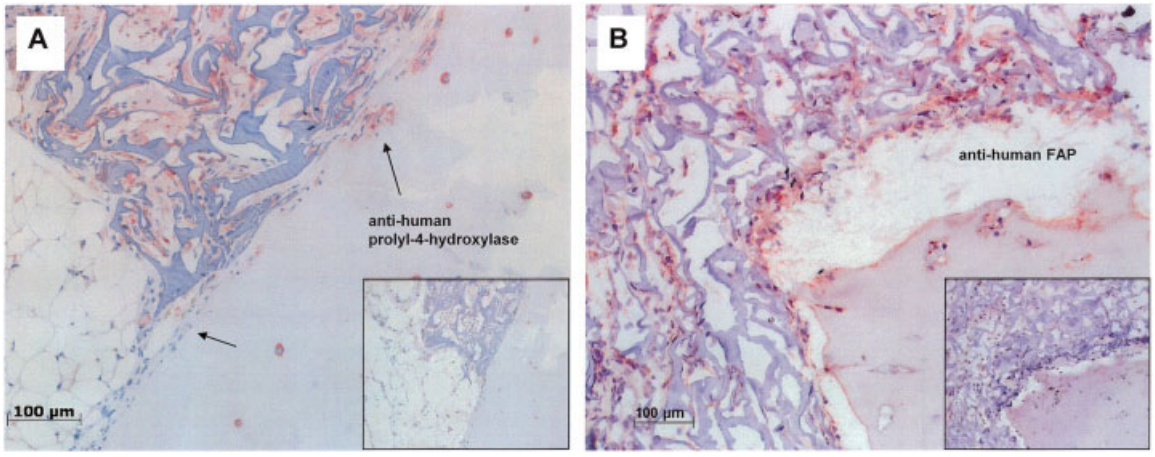

Figure 5. Invasive cells within cartilage degradation zones are FAP-expressing RASFs. Cartilage/sponge explants were analyzed immunohistochemically for human prolyl 4-hydroxylase (**A**) and human FAP (**B**). **Arrows** show unstained mouse cells and stained human RASFs. Positive signals appear in red. Nuclei were counterstained with hematoxylin. **Insets** show negative control slides (original magnification $\times$ 100). See Figure 1 for definitions.

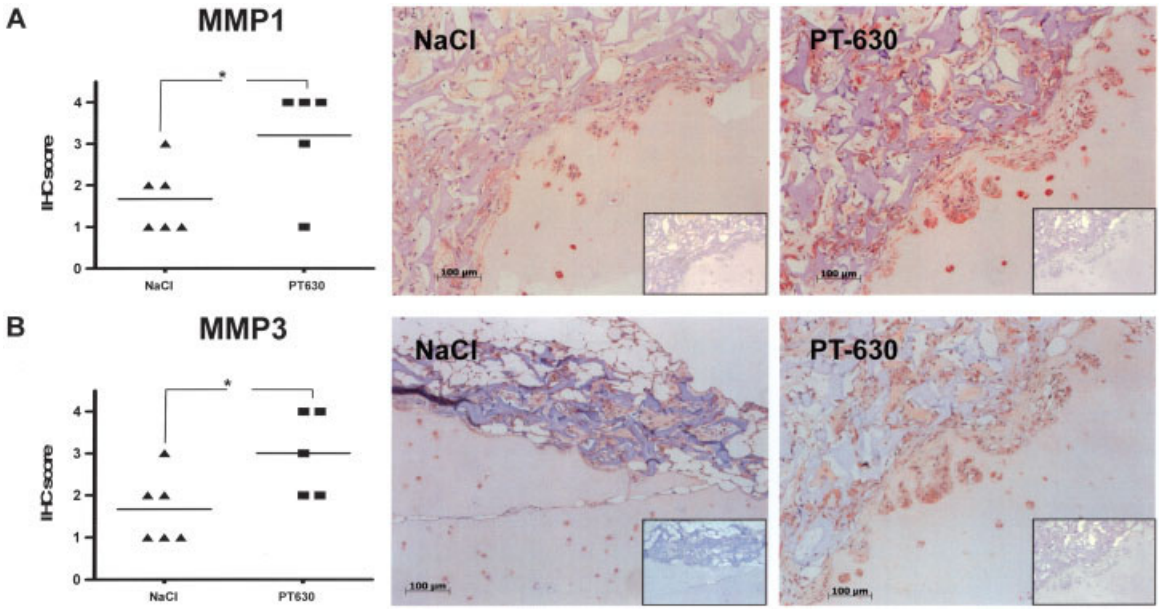

Figure 6. Inhibition of DPP-4–like activity enhances the release of matrix-degrading enzymes. Staining of matrix metalloproteinase 1 (MMP-1) (**A**) and MMP-3 (**B**) was assessed in controls (NaCl) and in mice treated with 50 μg PT-630 twice daily, and immunohistochemistry (IHC) scores were determined. Horizontal lines indicate the mean. $* = P < 0.05$ by 1-sample *t*-test. Photomicrographs are representative of experiments in 6 controls and in 5 PT-630–treated mice. Positive signals appear in red. Nuclei were counterstained with hematoxylin. **Insets** show negative control slides (original magnification $\times$ 100). See Figure 1 for other definitions.

and prompted us to investigate the triggering ligand. Increases in collagenase and gelatinase activity in the supernatants of cultured RASFs upon stimulation with SDF-1 (CXCL12), interferon-γ–inducible 10-kd protein (CXCL10), RANTES, and monokine induced by interferon-γ (CXCL9) have been described previously (30). These ligands share the X-Pro or X-Ala motif and are potential substrates for DPP-4–like activity (31). Isolation of N-terminally truncated chemokines from natural sources mainly suggests truncation of SDF-1 and RANTES in the presence of physiologic levels of DPP-4–like activity (32). While the expression levels of RANTES in the supernatants of cultured RASFs remained below the detection limit (15 pg/ml), levels of SDF-1 substantially increased after only 24 hours of treatment with PT-630, and the increase reached statistical significance after 48 hours (Figure 3C).

Inhibition of DPP-4–like activity promotes RASF invasion and cartilage degradation in vivo. The SCID mouse model of cartilage invasion is a unique in vivo model used to selectively study the invasion of human RASFs into human cartilage in a noninflammatory environment (33). We chose this model for the current study in order to determine whether inhibition of DPP-4–like activity upon oral treatment with PT-630 would also lead to the induction of MMPs in RASFs in vivo and would have an impact on the invasive behavior of implanted RASFs. After a treatment period of 60 days, the implants consisting of an inert sponge filled with RASFs and a piece of human cartilage were resected for histologic examination. As expected, synovial fibroblasts began to degrade the coimplanted cartilage of control mice receiving saline. However, in animals orally treated with PT-630, the cartilage was more strongly affected at places facing the sponge filled with RASFs (Figures 4A–C). This finding was reflected by a significantly higher invasion score of implants from mice treated with 50 μg PT-630 twice daily than from control mice (Figure 4D).

Immunohistochemical staining of the slides with anti-human prolyl 4-hydroxylase–specific antibodies confirmed that human RASFs invaded cartilage, whereas mouse cells, although attaching to the cartilage, were not invasive (Figure 5A). Additional staining revealed that invading cells were strongly FAP-positive in vivo (Figure 5B). Furthermore, consistent with our in vitro observations, staining of human MMP-1 and MMP-3 revealed significantly higher levels of matrix-

degrading enzymes at regions of RASF invasion and cartilage destruction following inhibition of serine protease activity, when compared with controls (Figures 6A and B).

DISCUSSION

The expression of FAP and DPP-4/CD26 in the RA synovium has begun attracting increased attention among investigators, since novel functions of extracellular serine proteases in the regulation of cell signaling (5) and modulation of inflammatory responses (34) have been recognized. Studies of how serine proteases contribute to the exacerbation of inflammatory processes in RA have mainly focused on the impact of CD26-dependent DPP activity associated with activated T cell functions (35). However, RASFs express not only DPP-4/CD26 but also FAP (12), and the peptidase activities of DPP-4/CD26 overlap with those of FAP (36).

In the current study, we demonstrated that, on cultured human RASFs, expression of FAP was stable and much stronger than expression of DPP-4/CD26. The fact that the cell surface expression pattern of DPP-4/CD26 is highly variable despite its stable gene transcription has been described previously (37) and is consistent with our findings. It has also been observed that cytokines regulate DPP-4/CD26 translation and maturation but not gene transcription (38). As expected, cell membrane–dependent serine protease activity of unstimulated RASFs could be detected for both FAP and DPP-4/CD26. This is important since prolyl peptidase activity is able to decrease the functionality of inflammation mediators by N-terminal cleavage. The observation that DPP-4/CD26 protein levels in synovial fluid are normal to low when compared with levels in controls (8) implies a lack of regulation of local levels of inflammatory cytokines by DPP-4/CD26 in RA patients. However, the higher protein levels of FAP on the surface of RASFs might compensate for lower levels of DPP-4/CD26, and the common membrane-tethered DPP-4–like activity might represent the supposed mechanism for counterregulation of inflammatory processes in RA synovium.

This is supported by our findings that inhibition of DPP-4–like activity upon treatment of RASFs with L-glutamyl L-boroproline (PT-630) increased levels of SDF-1 (CXCL12) in a time-and dose-dependent manner. Production of SDF-1 by RASFs has been reported to be crucially involved in maintaining the inflammatory process by recruitment of CXCR4-expressing T cells and monocytes from the periphery into the rheumatoid synovium (39). Furthermore, SDF-1 stimulates the release of MMP-3, MMP-9, and MMP-13 from chondrocytes that contribute to cartilage degradation (40,41). The half-life of active SDF-1 is controlled by N-terminal truncation in vivo (42). Cleavage of circulating active SDF-1 leads to reduced inflammation and cellular infiltration of the rheumatoid synovium (42) and could protect chondrocytes against cell death (43). However, the impact of SDF-1 at autocrine chemokine levels on the activation state and invasive behavior of RASFs was unknown. Herein, we demonstrate that inhibition of DPP-4–like activity increases autocrine SDF-1 levels, as well as MMP-1 and MMP-3. It has been recently reported that external stimulation of RASFs by SDF-1 at concentrations of ~100 ng/ml leads to increased collagenase activity. Irrespective of such high SDF-1 concentrations exceeding physiologic chemokine levels, total collagenase activity was measured by zymography, which does not differentiate between the activity of MMP-1 and MMP-13. Levels of MMP-3 were not investigated (30).

MMP-3 is a known activator of MMP-1, and up-regulation of both metalloproteinases resulting from DPP-4–like inhibition suggested a more aggressive phenotype of RASFs that would possibly enhance the degradation of cartilage collagen. To address this issue, we chose the SCID mouse coimplantation model, since the absence of inflammatory cells or inflammation mediators resulting from the SCID defect allowed us to specifically determine the impact of DPP-4–like activity on the invasive properties of RASFs (29,44). Invasion of xenotransplanted human RASFs into coimplanted human cartilage was significantly higher upon DPP-4–like inhibition, as compared with the invasion of RASFs with unaffected extracellular DPP-4–like activity. Invasive cells retaining FAP expression were of human origin. Regions of cartilage destruction from PT-630–treated mice were characterized by significantly higher accumulations of MMP-1 and MMP-3, as compared with controls. This is the first report describing the cartilage-protecting potential of DPP-4–like activity on human RASFs, and our findings highlight a substantial role of FAP in this process.

Our data are supported by the observation that antigen-induced arthritis is more severe in DPP-$4^{-/-}$ mice (42). However, DPP-4/CD26 also regulates biologic processes that are unrelated to its prolyl peptidase activity (e.g., cellular adhesion, cell differentiation, and apoptosis) (45). Consequently, DPP-4 gene silencing provokes complex phenotypic changes that hamper finding evidence of an exclusive linkage of the results gained

in the DPP-4–knockout model with abrogated DPP-4–like enzymatic activity. Above all, DPP-4–like activity mediated by other serine protease family members, particularly FAP, would remain unaffected in a DPP-$4^{-/-}$ animal model. The same group that reported findings from the DPP-$4^{-/-}$ mouse model also analyzed circulating prolyl peptidase activity in plasma from RA patients. Enzymatic activity levels in the plasma and DPP-4/CD26 antigen levels in the blood were significantly decreased in RA patients. Reduced levels negatively correlated with levels of C-reactive protein, a parameter for inflammatory disease activity in RA patients (42). However, that report focused on DPP-4/CD26 prolyl peptidase activity and did not mention cell membrane DPP-4–like activity of RASFs.

In contrast to our findings, competitive DPP-4/CD26 inhibition has been reported to suppress arthritis development in rat collagen-induced arthritis models. However, the DPP-4/CD26 inhibitor used was also effective in DPP-4–deficient rats, which suggests varied targeting for this drug (46). Similar effects have been observed after administration of prolyl peptidase inhibitors for tumor therapy. A compound with potent activity against several tumor entities remained active in DPP-$4^{-/-}$ mice (47) and is now known to inhibit cytoplasmic prolyl peptidases DPP-8 and DPP-9 as well, thereby inducing a cytokine-mediated immunologic response (48).

Consistent with our findings, increased expression of SDF-1 also promoted ECM degradation and migration of tumor cells (49). Upon malignant transformation, down-regulation or even loss of DPP-4/CD26 on tumor cells contributes to a more aggressive phenotype. In contrast, restoration of neuroblastoma cells with DPP-4/CD26 suppressed tumor growth in nude mice by down-regulation of SDF-1 signaling (45). These data support the notion of a potential inhibitory role for prolyl peptidase activity on the progression of invasive diseases. Independent of DPP-4–like activity, DPP-4/CD26 and FAP display further activities within connective tissues. Of note, the interaction between collagen and DPP-4/CD26 is mediated by residues in the cysteine-rich region of the protein and not by the catalytic domain (50). Coexpression of DPP-4/CD26 and FAP results in the formation of heterodimeric complexes on the cell surface (16), and complex formation at invadopodia of migrating fibroblasts is required for cell invasion on a type I collagen matrix (17). This highlights the need for further investigations focusing on the complex interaction of these proteases among themselves and with components of the ECM.

In summary, our results strongly support the notion of a pivotal role for cell surface DPP-4–like activity as a potential protective factor against invasion by RASFs and degradation of joint cartilage. These findings provide deeper insight into the spectrum of DPP-4/CD26– and FAP-dependent activities upon their expression in rheumatoid synovium. Moreover, our data lay the groundwork for therapeutic strategies targeting the noncatalytic functions of DPP-4/CD26 or FAP and for the development of novel routes for treatment of RA.

ACKNOWLEDGMENTS

We thank Maria Comazzi, Ferenc Pataky, and Nadja Jaouad for their excellent technical support and Dr. Ellen Pure for assistance with the animal model.

AUTHOR CONTRIBUTIONS

All authors were involved in drafting the article or revising it critically for important intellectual content, and all authors approved the final version to be published. Dr. Bauer had full access to all of the data in the study and takes responsibility for the integrity of the data and the accuracy of the data analysis.

Study conception and design. Ospelt, Jüngel, Knuth, R. Gay, Michel, S. Gay, Renner, Bauer.

Acquisition of data. Ospelt, Mertens, Brentano, Maciejewska-Rodriguez, Huber, Hemmatazad, Bauer.

Analysis and interpretation of data. Ospelt, Wüest, Bauer.

REFERENCES

1. Huber LC, Distler O, Tarner I, Gay RE, Gay S, Pap T. Synovial fibroblasts: key players in rheumatoid arthritis. Rheumatology (Oxford) 2006;45:669–75.
2. Tomita T, Nakase T, Kaneko M, Shi K, Takahi K, Ochi T, et al. Expression of extracellular matrix metalloproteinase inducer and enhancement of the production of matrix metalloproteinases in rheumatoid arthritis. Arthritis Rheum 2002;46:373–8.
3. Morimoto C, Lord CI, Zhang C, Duke-Cohan JS, Letvin NL, Schlossman SF. Role of CD26/dipeptidyl peptidase IV in human immunodeficiency virus type 1 infection and apoptosis. Proc Natl Acad Sci U S A 1994;91:9960–4.
4. Rettig WJ, Garin-Chesa P, Beresford HR, Oettgen HF, Melamed MR, Old LJ. Cell-surface glycoproteins of human sarcomas: differential expression in normal and malignant tissues and cultured cells. Proc Natl Acad Sci U S A 1988;85:3110–4.
5. Kelly T. Fibroblast activation protein-α and dipeptidyl peptidase IV (CD26): cell-surface proteases that activate cell signaling and are potential targets for cancer therapy. Drug Resist Updat 2005;8:51–8.
6. Rasmussen HB, Branner S, Wiberg FC, Wagtmann N. Crystal structure of human dipeptidyl peptidase IV/CD26 in complex with a substrate analog. Nat Struct Biol 2003;10:19–25.
7. Muscat C, Bertotto A, Agea E, Bistoni O, Ercolani R, Tognellini R, et al. Expression and functional role of 1F7 (CD26) antigen on peripheral blood and synovial fluid T cells in rheumatoid arthritis patients. Clin Exp Immunol 1994;98:252–6.
8. Cordero OJ, Salgado FJ, Mera-Varela A, Nogueira M. Serum interleukin-12, interleukin-15, soluble CD26, and adenosine

deaminase in patients with rheumatoid arthritis. Rheumatol Int 2001;21:69–74.
9. Kamori M, Hagihara M, Nagatsu T, Iwata H, Miura T. Activities of dipeptidyl peptidase II, dipeptidyl peptidase IV, prolyl endopeptidase, and collagenase-like peptidase in synovial membrane from patients with rheumatoid arthritis and osteoarthritis. Biochem Med Metab Biol 1991;45:154–60.
10. Kullertz G, Boigk J. Dipeptidyl peptidase IV activity in the serum and synovia of patients with rheumatoid arthritis. Z Rheumatol 1986;45:52–6.
11. Fujita K, Hirano M, Ochiai J, Funabashi M, Nagatsu I, Nagatsu T, et al. Serum glycylproline p-nitroanilidase activity in rheumatoid arthritis and systemic lupus erythematosus. Clin Chim Acta 1978; 88:15–20.
12. Bauer S, Jendro MC, Wadle A, Kleber S, Stenner F, Dinser R, et al. Fibroblast activation protein is expressed by rheumatoid myofibroblast-like synoviocytes. Arthritis Res Ther 2006;8:R171.
13. Milner JM, Kevorkian L, Young DA, Jones D, Wait R, Donell ST, et al. Fibroblast activation protein α is expressed by chondrocytes following a pro-inflammatory stimulus and is elevated in osteoarthritis. Arthritis Res Ther 2006;8:R23.
14. Lee KN, Jackson KW, Christiansen VJ, Lee CS, Chun JG, McKee PA. Antiplasmin-cleaving enzyme is a soluble form of fibroblast activation protein. Blood 2006;107:1397–404.
15. Aertgeerts K, Levin I, Shi L, Snell GP, Jennings A, Prasad GS, et al. Structural and kinetic analysis of the substrate specificity of human fibroblast activation protein α. J Biol Chem 2005;280: 19441–4.
16. Scanlan MJ, Raj BK, Calvo B, Garin-Chesa P, Sanz-Moncasi MP, Healey JH, et al. Molecular cloning of fibroblast activation protein α, a member of the serine protease family selectively expressed in stromal fibroblasts of epithelial cancers. Proc Natl Acad Sci U S A 1994;91:5657–61.
17. Ghersi G, Dong H, Goldstein LA, Yeh Y, Hakkinen L, Larjava HS, et al. Regulation of fibroblast migration on collagenous matrix by a cell surface peptidase complex. J Biol Chem 2002;277: 29231–41.
18. Aggarwal S, Brennen WN, Kole TP, Schneider E, Topaloglu O, Yates M, et al. Fibroblast activation protein peptide substrates identified from human collagen I derived gelatin cleavage sites. Biochemistry 2008;47:1076–86.
19. Christiansen VJ, Jackson KW, Lee KN, McKee PA. Effect of fibroblast activation protein and α2-antiplasmin cleaving enzyme on collagen types I, III, and IV. Arch Biochem Biophys 2007;457: 177–86.
20. Vanhoof G, Goossens F, De Meester I, Hendriks D, Scharpe S. Proline motifs in peptides and their biological processing. FASEB J 1995;9:736–44.
21. Arnett FC, Edworthy SM, Bloch DA, McShane DJ, Fries JF, Cooper NS, et al. The American Rheumatism Association 1987 revised criteria for the classification of rheumatoid arthritis. Arthritis Rheum 1988;31:315–24.
22. Bauer S, Adrian N, Williamson B, Panousis C, Fadle N, Smerd J, et al. Targeted bioactivity of membrane-anchored TNF by an antibody-derived TNF fusion protein. J Immunol 2004;172: 3930–9.
23. Park JE, Lenter MC, Zimmermann RN, Garin-Chesa P, Old LJ, Rettig WJ. Fibroblast activation protein, a dual specificity serine protease expressed in reactive human tumor stromal fibroblasts. J Biol Chem 1999;274:36505–12.
24. Pure E. The road to integrative cancer therapies: emergence of a tumor-associated fibroblast protease as a potential therapeutic target in cancer. Expert Opin Ther Targets 2009;13:967–73.
25. Cheng JD, Valianou M, Canutescu AA, Jaffe EK, Lee HO, Wang H, et al. Abrogation of fibroblast activation protein enzymatic activity attenuates tumor growth. Mol Cancer Ther 2005;4:351–60.
26. Ospelt C, Kurowska-Stolarska M, Neidhart M, Michel BA, Gay RE, Laufer S, et al. The dual inhibitor of lipoxygenase and cyclooxygenase ML3000 decreases the expression of CXCR3 ligands. Ann Rheum Dis 2008;67:524–9.
27. Distler JH, Jungel A, Huber LC, Seemayer CA, Reich CF III, Gay RE, et al. The induction of matrix metalloproteinase and cytokine expression in synovial fibroblasts stimulated with immune cell microparticles. Proc Natl Acad Sci U S A 2005;102:2892–7.
28. Narra K, Lee HO, Lerro A, Valvardi J, Azeez O, Jesson MI, et al. Inhibitors of the stromal protease fibroblast activation protein attenuate tumor growth in vivo. AACR Meeting Abstracts 2006; 2006:1029.
29. Muller-Ladner U, Kriegsmann J, Franklin BN, Matsumoto S, Geiler T, Gay RE, et al. Synovial fibroblasts of patients with rheumatoid arthritis attach to and invade normal human cartilage when engrafted into SCID mice. Am J Pathol 1996;149:1607–15.
30. Garcia-Vicuna R, Gomez-Gaviro MV, Dominguez-Luis MJ, Pec MK, Gonzalez-Alvaro I, Alvaro-Gracia JM, et al. CC and CXC chemokine receptors mediate migration, proliferation, and matrix metalloproteinase production by fibroblast-like synoviocytes from rheumatoid arthritis patients. Arthritis Rheum 2004;50:3866–77.
31. Lambeir AM, Proost P, Durinx C, Bal G, Senten K, Augustyns K, et al. Kinetic investigation of chemokine truncation by CD26/dipeptidyl peptidase IV reveals a striking selectivity within the chemokine family. J Biol Chem 2001;276:29839–45.
32. Shioda T, Kato H, Ohnishi Y, Tashiro K, Ikegawa M, Nakayama EE, et al. Anti-HIV-1 and chemotactic activities of human stromal cell-derived factor 1α (SDF-1α) and SDF-1β are abolished by CD26/dipeptidyl peptidase IV-mediated cleavage. Proc Natl Acad Sci U S A 1998;95:6331–6.
33. Pierer M, Muller-Ladner U, Pap T, Neidhart M, Gay RE, Gay S. The SCID mouse model: novel therapeutic targets—lessons from gene transfer. Springer Semin Immunopathol 2003;25:65–78.
34. Pham CT. Neutrophil serine proteases: specific regulators of inflammation. Nat Rev Immunol 2006;6:541–50.
35. Sedo A, Duke-Cohan JS, Balaziova E, Sedova LR. Dipeptidyl peptidase IV activity and/or structure homologs: contributing factors in the pathogenesis of rheumatoid arthritis? Arthritis Res Ther 2005;7:253–69.
36. Edosada CY, Quan C, Wiesmann C, Tran T, Sutherlin D, Reynolds M, et al. Selective inhibition of fibroblast activation protein protease based on dipeptide substrate specificity. J Biol Chem 2006;281:7437–44.
37. Mattern T, Reich C, Duchrow M, Ansorge S, Ulmer AJ, Flad HD. Antibody-induced modulation of CD26 surface expression. Immunology 1995;84:595–600.
38. Salgado FJ, Vela E, Martin M, Franco R, Nogueira M, Cordero OJ. Mechanisms of CD26/dipeptidyl peptidase IV cytokine-dependent regulation on human activated lymphocytes. Cytokine 2000; 12:1136–41.
39. Seki T, Selby J, Haupl T, Winchester R. Use of differential subtraction method to identify genes that characterize the phenotype of cultured rheumatoid arthritis synoviocytes. Arthritis Rheum 1998;41:1356–64.
40. Kanbe K, Takagishi K, Chen Q. Stimulation of matrix metalloprotease 3 release from human chondrocytes by the interaction of stromal cell–derived factor 1 and CXC chemokine receptor 4. Arthritis Rheum 2002;46:130–7.
41. Chiu YC, Yang RS, Hsieh KH, Fong YC, Way TD, Lee TS, et al. Stromal cell-derived factor-1 induces matrix metalloprotease-13 expression in human chondrocytes. Mol Pharmacol 2007;72: 695–703.
42. Busso N, Wagtmann N, Herling C, Chobaz-Peclat V, Bischof-Delaloye A, So A, et al. Circulating CD26 is negatively associated with inflammation in human and experimental arthritis. Am J Pathol 2005;166:433–42.
43. Wei L, Sun X, Kanbe K, Wang Z, Sun C, Terek R, et al. Chondrocyte death induced by pathological concentration of

chemokine stromal cell-derived factor-1. J Rheumatol 2006;33: 1818–26.
44. Muller-Ladner U, Pap T, Gay RE, Gay S. Gene transfer as a future therapy for rheumatoid arthritis. Expert Opin Biol Ther 2003;3:587–98.
45. Arscott WT, LaBauve AE, May V, Wesley UV. Suppression of neuroblastoma growth by dipeptidyl peptidase IV: relevance of chemokine regulation and caspase activation. Oncogene 2009;28: 479–91.
46. Tanaka S, Murakami T, Horikawa H, Sugiura M, Kawashima K, Sugita T. Suppression of arthritis by the inhibitors of dipeptidyl peptidase IV. Int J Immunopharmacol 1997;19:15–24.
47. Adams S, Miller GT, Jesson MI, Watanabe T, Jones B, Wallner BP. PT-100, a small molecule dipeptidyl peptidase inhibitor, has potent antitumor effects and augments antibody-mediated cytotoxicity via a novel immune mechanism. Cancer Res 2004; 64:5471–80.
48. Hu Y, Ma L, Wu M, Wong MS, Li B, Corral S, et al. Synthesis and structure-activity relationship of N-alkyl Gly-boro-Pro inhibitors of DPP4, FAP, and DPP7. Bioorg Med Chem Lett 2005;15: 4239–42.
49. Raman D, Baugher PJ, Thu YM, Richmond A. Role of chemokines in tumor growth. Cancer Lett 2007;256:137–65.
50. Loster K, Zeilinger K, Schuppan D, Reutter W. The cysteine-rich region of dipeptidyl peptidase IV (CD 26) is the collagen-binding site. Biochem Biophys Res Commun 1995;217:341–8.